applied sciences

MDPI

Article

Characterization and Evaluation of Commercial Carboxymethyl Cellulose Potential as an Active Ingredient for Cosmetics

Eduardo M. Costa, Carla F. Pereira, Alessandra A. Ribeiro, Francisca Casanova, Ricardo Freixo, Manuela Pintado and Oscar L. Ramos *

Universidade Católica Portuguesa, CBQF—Centro de Biotecnologia e Química Fina—Laboratório Associado, Escola Superior de Biotecnologia, Rua Diogo Botelho 1327, 4169-005 Porto, Portugal; emcosta@porto.ucp.pt (E.M.C.); cpfpereira@ucp.pt (C.F.P.); abribeiro@ucp.pt (A.A.R.); fcbastos@ucp.pt (F.C.); rfreixo@ucp.pt (R.F.); mpintado@ucp.pt (M.P.)
* Correspondence: oramos@ucp.pt

Abstract: Carboxymethyl cellulose is the most used water-soluble cellulose with applications in industries such as food, cosmetics, and tissue engineering. However, due to a perceived lack of biological activity, carboxymethyl cellulose is mostly used as a structural element. As such, this work sought to investigate whether CMC possesses relevant biological properties that could grant it added value as a cosmeceutical ingredient in future skincare formulations. To that end, CMC samples (M_w between 471 and 322 kDa) skin cell cytotoxicity, impact upon pro-collagen I α I production, and inflammatory response were evaluated. Results showed that samples were not cytotoxic towards HaCat and HDFa up to 10 mg/mL while simultaneously promoting intracellular production of pro-collagen I α I up by 228% relative to the basal metabolism, which appeared to be related to the highest DS and M_w. Additionally, CMC samples modulated HaCat immune response as they decreased by ca. 1.4-fold IL-8 production and increased IL-6 levels by ca. five fold. Despite this increase, only two samples presented IL-6 levels similar to those of the inflammation control. Considering these results, CMC showed potential to be a more natural alternative to traditional bioactive cosmetic ingredients and, as it is capable of being a bioactive and structural ingredient, it may play a key role in future skincare formulations.

Keywords: carboxymethyl cellulose; cosmeceutical; skin keratinocytes; skin normal fibroblasts; immunomodulation; pro-collagen production

Citation: Costa, E.M.; Pereira, C.F.; Ribeiro, A.A.; Casanova, F.; Freixo, R.; Pintado, M.; Ramos, O.L. Characterization and Evaluation of Commercial Carboxymethyl Cellulose Potential as an Active Ingredient for Cosmetics. *Appl. Sci.* **2022**, *12*, 6560. https://doi.org/10.3390/app12136560

Academic Editor: Manoj Gupta

Received: 23 May 2022
Accepted: 27 June 2022
Published: 28 June 2022

1. Introduction

Polysaccharides are one of the most abundant bioactive inexpensive substances found in nature and have long been used in food, cosmetics, and pharmaceutical industries. Carboxymethyl cellulose (CMC) is the most produced and industrially used water-soluble cellulose derivative [1,2]. It is commonly produced by a Williamson etherification, with the first step consisting of the modification of cellulose by sodium hydroxide to obtain the sodium cellulosate. This is followed by the production of sodium chloroacetate via the dissolution of chloroacetic acid in sodium hydroxide, which will prompt the reaction of the chlorine in the sodium chloroacetate with the sodium cellulosate to produce CMC [3]. By definition, CMC is a copolymer constituted by two units—β-D-glucose and β-D-glucopyranose 2-*O*-(carboxymethyl)-monosodium salt linked by β-1,4-glycosidic bonds. The insertion of carboxymethyl groups (-CH_2-COOH) on the glucose residues in the cellulose backbone improves its interfacial characteristics, providing CMC with a vast array of properties among which are thickener, suspending aid, binder, film-former, gelling agent, stabilizer, water retention agent, protective colloid, and rheology control agent, thus allowing its applicability in very distinctive industries such as food, cosmetic, pharmaceutical, and biomedical [4–6]. The beneficial inherent properties of CMC, in particular, its lack of

toxicity, high stability, pH sensitivity, biodegradability, and biocompatibility, has opened new fields of application with studies showing its potential in advanced fields such as tissue engineering, bone-tissue engineering, and wound dressing [6–10].

When one considers the industrial applications of CMC there are various patents describing the application in wound dressings [11], drug delivery [12], and cosmetics [13]. For cosmetics in particular, polysaccharides and CMC are widely described as being fundamental for the development of personal care formulations. Their compatibility with other ingredients, safety, and diverse nature (cationic, anionic or amphoteric charge) makes them prime candidates to be modified and incorporated in formulations as moisturizers, hydrators, and emulsifiers [14]. CMC, in particular, has been reported as being used as a rheological modifier for hair conditioners and hair styling products; as a replacer for surfactants in formulations while simultaneously working as an emulsifying, thickening, and stabilizing agent; and as structural ingredient in creams, lotions, and gels [15–17]. One example in particular has been given by Martins and Rocha [15] where CMC, in conjunction with bacterial cellulose, was used as an emulsifier in an oil-in-water generic cosmetic cream and was capable of fully replacing commercial surfactants and maintained rheological properties of the formulations. Another example can be found in the work of Wongkom and Jimtaisong [18] where the use of CMC as a delivery matrix for hydrophilic sunscreens was described. In addition to these structural characteristics, CMC, as polymer, is less sensitive to microbial contaminations than other natural or synthetic gelling agents, thus extending the personal care formulations' shelf life [17].

Taking in consideration the above information, one fact stands out: CMC has always been described as a structural agent valued for its capacity to be compatible with other bioactive ingredients that are responsible for the formulation's biological activity. However, scarce information is available in the literature reporting CMC activity as a bioactive ingredient, and no information at all can be found exploring its potential in the modulation of collagen synthesis or its role in inflammatory response. Moreover, this paper goes beyond the others by trying to establish a correlation between the biological properties screened and the CMC physicochemical and structural properties that were also evaluated here. Thus, considering the ubiquitous nature of CMC in cosmetic formulations we hypothesize that CMC will demonstrate biological activity that can add value and potentiate the usage of CMC in personal care formulations. Therefore, to unlock this potential we sought to produce, for the first time, a full image of CMC's capacity to modulate the production of skin metabolite which is critical for most cosmetic formulations—collagen. To that end, four different commercially available CMC samples had their intrinsic physicochemical and structural properties characterized and were then evaluated for their biocompatibility towards skin keratinocytes and fibroblasts, impact upon pro-collagen I-α-I production in fibroblasts and modulation of inflammatory response through the evaluation of interleukin-6 and 8 using an HaCat inflammation model. With these data we try to prove for the first time that CMC is a viable alternative for traditional collagen promoting ingredients and that it can in fact perform a dual role in personal care formulations, being simultaneously a structural and a bioactive ingredient.

2. Materials and Methods

The evaluation of CMC's potential was performed according to the scheme detailed in Figure 1, with information regarding the materials and methods used being given bellow.

2.1. CMC Samples

Three commercially available plant cellulose derived sodium carboxymethyl cellulose samples were acquired from key manufacturers and suppliers worldwide. The samples were coded as CMC1, CMC2, and CMC3. A standard CMC (hereinafter referred to as CMC4) with a degree of substitution of 0.7 purchased from Sigma-Aldrich was used as a comparative control. Chemicals were reagent-grade or better and were used without further purification.

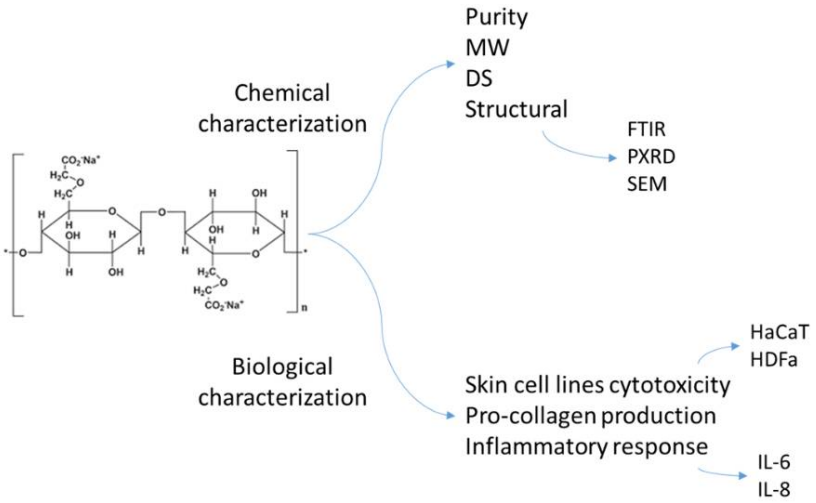

Figure 1. Scheme showing the experimental procedure taken to analyze CMC's cosmeceutical potential.

2.2. CMC Solutions Preparation

Stock solutions at 20 g/mL were prepared by dissolving each CMC powder sample in deionized water and left stirring at room temperature until complete dissolution as follows: 20 ± 0.1 g of each CMC sample was used "as-received" with a careful and slow addition to deionized water at 25 °C to assure a good dispersion. The solutions were then gently stirred for 4 h after which the pH was adjusted to 6.5–7.5 using 0.1 M NaOH or 0.1 M HCl, as appropriate, to minimize the possible impact of pH.

2.3. CMC Samples Characterization

2.3.1. Structural Characterization

The structural analysis of CMC samples was attained by Fourier Transform Infrared Spectroscopy (FT-IR), Powder X-ray Diffraction (PXRD), and Scanning Electron Microscopy (SEM).

The FT-IR spectra were recorded using the Frontier™ MIR/FIR spectrometer from PerkinElmer in a scanning range of 550–4000 cm^{-1} for 16 scans at a spectral resolution of 4 cm^{-1}. All analyses were done in triplicate.

Powder X-ray Diffraction Analysis (PXRD) was performed on Rigaku MiniFlex 600 diffractometer with Cu kα radiation, with a voltage of 40 kV and a current of 15 mA ($3° \leq 2\theta \geq 60°$; a step of 0.01 and speed rate of 3.0°/min). The evaluation of the crystallinity index (%CI) was performed based on the profile and the baseline adjustment of the diffractogram based on reflection areas by amorphous subtraction using the program PDXL2 from Rigaku® (version 2.8.1.1). All measurements were done in duplicate.

The morphology of CMC samples was evaluated by Scanning Electron Microscopy (SEM) on JSM-5600 LV Scanning Electron Microscope from JEOL, Tokyo, Japan. Before analysis, the CMC powdered samples were placed in observation stubs (covered with double-sided adhesive carbon tape (NEM tape, Nisshin, Japan) and coated with Aug/Pd using a Sputter Coater (Polaron, Bad Schwalbach, Germany). All observations were performed in high-vacuum with an acceleration voltage of 30 kV, at a working distance of 9–10 mm and a spot size of 4. The images presented here are representative images of the morphology of each sample.

2.3.2. Purity

The purity of all CMC samples was evaluated according to the standard method D1439-15 [19]. Briefly, 3 ± 0.1 g of each sample "as-received" to the nearest 0.001 g was placed in a beaker and stirred with two portions of 150 mL of ethanol at 60 °C (80% v/v) for 15 min. The supernatant was properly decanted at the end of each step. The undissolved

matter was then dried and weighed to calculate the percentage of CMC, on a dry weight basis, according to the following equation:

$$\%CMC = (A \times 10{,}000)/(B\,(100 - C)) \quad (1)$$

where: A = mass of dried residue (g); B = mass of sample used (g) and C = moisture in the sample as received (%). All assays were performed in duplicate.

The moisture content was also studied according to the same method [19]. Briefly, each CMC sample was placed in a crucible and heated in a convection oven at 105 °C for 2 h. Each crucible was then placed in a desiccator, covered with flat glass, cooled to room temperature and weighed. This procedure was continuously performed for periods of 1 h until the mass loss did not exceed 0.003 g. The determination of moisture content was performed in duplicate for each sample.

2.3.3. Degree of Substitution

The absolute values of the Degree of Substitution (DS) of all CMC samples were determined using potentiometric back-titration by the ASTM D1439-15 standard method in duplicate assays for each sample [19]. According to this method, approximately 4 g of each powdered sample placed in 75 mL of ethanol (95%, v/v) were stirred at room temperature for 10 min, followed by the addition of 5 mL of HNO_3, under stirring. The slurry was then boiled for 5 min. At the end of this step, the solution was removed from the heat and continuously stirred further for 15 min. The liquid supernatant was decanted, and the precipitate was washed with 30 mL of ethanol (80%, v/v) previously heated to 60 °C. This step was repeated five times. Next, the precipitate was further washed with anhydrous methanol, filtered, and dried at 105 °C for 3 h, followed by cooling in a desiccator for 40 min. For titration purposes (repeated twice), about 0.5 g (nearest to 0.01 g) of each dried acid CMC was dissolved in 100 mL of distilled water. Then, 25.00 mL of 0.3 N NaOH solution was added, under stirring, and the solution was heated to a boil and boiled for 15 min. The excess NaOH was titrated with 0.3 N HCl, using phenolphthalein as an indicator, while the solution was still hot. The DS was calculated using Equations (2) and (3), as follows:

$$A = \frac{[(BC) - (DE)]}{F} \quad (2)$$

$$DS = \frac{0.162A}{1 - (0.058A)} \quad (3)$$

where A = milliequivalents of acid consumed per gram of sample; B = NaOH solution added (mL); C = normality of NaOH solution; D = HCl solution required for titration (mL); E = normality of HCl solution; F = weight of sample (g); 162 = gram molecular mass of the anhydroglucose unit of cellulose; and 58 = MW of carboxymethyl group.

2.3.4. Average Molecular Weight

Chromatographic analyses were performed on the liquid chromatograph Agilent 1260 Infinity II LC System apparatus equipped with the Agilent 1290 Infinity II Evaporative Light Scattering Detector (N2 Flow: 1.2 SLM; Evaporator temperature: 70 °C and Nebulizer Temperature: 50 °C). PL aquagel-OH MIXED-M (PN: PL1149-6801—4.6 × 250 mm, 8 µm) and Aquagel-OH 20 (PN: PL1120-6520 300 × 7.5 mm, 5 µm) and a pre-column (PL aquagel-OH PN: PL1149-1240 PL aquagel-OH, 7.5 × 50 mm, 15 µm) were used. The analyses performed in triplicate for each CMC sample were carried out using ammonium acetate (10 mM) as solvent and eluent with a flow rate of 0.6 mL min^{-1}. CMC solutions at 1% (w/v) in ammonium acetate (10 mM) were previously filtered through a 0.2 µm filter. All chromatograms were analyzed using the OpenLab ChemStation program. The Shodex standards (P-82 kit; Cat. #: WAT034207: P-800 (MW = 736 kDa); P-400 (MW = 348 kDa); P-200 (MW = 200 kDa); P-100 (MW = 113 kDa); P-50 (MW = 49 kDa); P-20 (MW = 23 kDa); P-10 (MW = 9.9 kDa) and P-5 (MW = 6.6 kDa)) used for the calibration curve in order to

obtain the molar mass distribution were obtained from Waters Chromatography (Madrid, Spain). The transformation of the chromatographic data into a molar mass distribution implies the determination of the following parameters: (i) weight-average molar mass (M_W); number-average molar mass (Mn); and polydispersity index (PI) [20–22]. The average molecular weights and I based on the peak area of each fraction (Ai) selected in each chromatogram are defined according to Equations (4)–(6):

$$M_w = \left(\Sigma A_i M_i^2\right) / (\Sigma A_i M_i) \quad (4)$$

$$M_n = (\Sigma A_i M_i) / (\Sigma A_i) \quad (5)$$

$$I = M_w / M_n \quad (6)$$

2.4. Cell Lines and Culture Conditions

Two different cell lines were assayed throughout this work. Human keratinocytes—HaCaT (CLS 300493, Eppelheim, Germany) and Primary Dermal Fibroblasts, normal, human, and adult—HDFa (ATCC PCS-201-012, Manassas, VA, USA). HaCat cells were cultured at 37 °C in a humidified atmosphere of 95% air and 5% CO_2, as monolayers using Dulbecco's Modified Eagle's Medium (DMEM) with 4.5 g/L glucose, L-glutamine without pyruvate (ThermoScientific, Waltham, MA, USA) containing 10% fetal bovine serum (ThermoScientific, Waltham, MA, USA) and 1% (v/v) Penicillin-Streptomycin-Fungizone (ThermoScientific, Waltham, MA, USA). HDFa cells were cultured at 37 °C in a humidified atmosphere of 95% air and 5% CO_2, as monolayers using Fibroblast Growth Medium (Sigma-Aldrich, St. Louis, MO, USA). Keratinocytes were used between passages 35 and 41 and fibroblasts were used between passages 7 and 9.

2.5. Cytotoxicity Evaluation

Cytotoxicity evaluation was performed according to the ISO 10993-5:2009 standard in HaCaT and HDFa cells [23]. Cells were grown to 80–90% confluence, detached using TrypLE Express (ThermoScientific, Waltham, MA, USA), and seeded at 1×10^4 cells/well in a 96-well microplate (Nunclon Delta, ThermoScientific, Waltham, MA, USA). After 24 h the culture media was carefully removed and replaced with culture media supplemented with CMC at concentrations between 0.31 and 10 mg/mL. DMSO (Sigma, St. Louis, MO, USA) at 10% (v/v) in culture media was used as a death control and plain culture media was used as growth control. After 24 h of incubation, 10 µL of Presto Blue (Thermofisher, Waltham, MA, USA) was added to each well and incubated for 1 h. After this period, fluorescence (Ex: 560 nm; Em: 590 nm) was measured using a microplate reader (Synergy H1, Biotek Instruments, Winooski, VT, USA). All assays were performed in quadruplicate.

2.6. Pro-Collagen I α I Biosynthesis and Quantification

2.6.1. Pro-Collagen I α I Biosynthesis

HDFa cells were grown to 80–90% confluence, detached using TrypLE Express, seeded at 5×10^5 cells/well in a 6-well microplate (Corning, New York, NY, USA), and incubated for 24 h at 37 °C in a humidified atmosphere of 95% air and 5% CO_2. After 24 h, the culture media was carefully replaced with CMC (at the highest non-cytotoxic concentration) supplemented media and the plate was re-incubated for another 24 h. At the end of the assay, supernatants were collected, centrifuged to remove debris, and stored for further analysis. Cells were washed with chilled PBS and cell extracts were obtained using the Human Pro-Collagen I alpha1 Catchpoint SimpleStep Elisa (Abcam, Cambridge, MA, USA) according to the manufacturer's instructions. The protein content of aliquots of cells extracts was determined using the BCA Pierce Assay Kit (ThermoScientific, Waltham, MA, USA). All biosynthesis assays were performed in quadruplicate.

2.6.2. Pro-Collagen I α I Quantification

The concentration of pro-collagen I α I in supernatants and cell extracts samples was determined by enzyme-linked immunosorbent assay (ELISA) using the Human Pro-Collagen I alpha1 Catchpoint SimpleStep Elisa (Abcam, Cambridge, MA, USA) according to the manufacturer's instructions. Cell extracts data were normalized to the sample protein content and cell supernatants were diluted 50× prior to analysis. The pro-collagen content of the control group was set to 100%. All assays were performed in quadruplicate.

2.7. Inflammatory Response

Evaluation of Interleukin-6 and interleukin-8 production in HaCaT was used to evaluate the CMC's effect on the cellular inflammatory response. This assay was performed by enzyme-linked immunosorbent assay (ELISA) using the Human IL-6 Elisa Max Standard Set and the Human IL-8 Elisa Max Standard Set (BioLegend, San Diego, CA, USA) according to the manufacturer's instructions. CMC was used at the highest non-cytotoxic concentration. Basal levels of production were used as non-stimulated control. Lipopolysaccharides from Escherichia coli (serotype O55:B5) (LPS) (Sigma-Aldrich, St. Louis, MO, USA) at 1 µg/mL was used as a pro-inflammation control. All assays were performed in quadruplicate.

2.8. Statistical Analysis

Statistical analysis was performed using IBM SPSS Statistics v21.0.0 (New York, NY, USA) software. As the data followed a normal distribution, one-way ANOVA coupled with Tukey's post hoc test was used to assess the differences between the results observed with differences being considered significant for p-values below 0.05.

3. Results and Discussion

3.1. Carboxymethylcellulose Characterization

The structural and physical properties of all CMC samples (1–4) was performed using standard methodologies. The real core of this section consists of the analysis of all samples according to the same methodology to obtain standard and accurate information on all properties of different samples that may have a putative impact on the study of the biological properties.

3.1.1. Structural Analysis

The results of the samples structural analysis can be seen in Figure 2.

The normalized FT-IR spectra of studied CMCs highlighted in Figure 2b exhibited three strong absorption bands at 1318, 1417, and 1591 cm^{-1} assigned to the bending vibration of O-H group, CH_2 scissoring, and COO-asymmetrical stretching, respectively, characteristic of the carboxymethyl functional group [24]. The broad peak at 2980–3680 cm^{-1} is attributed to the –OH from the carboxymethyl functional group and to the O-H stretching from the glucose ring, while the weak absorption band at 2882–2984 cm^{-1} indicates the C-H stretching vibration within the glucose unit [24,25]. The absorption peak at 1023 cm^{-1} is associated with the C-O stretching vibration and the absorption peak at 899 cm^{-1} is assigned to the glycosidic –C1-H stretching [24].

The analysis of the powder X-ray diffraction patterns of the four CMC samples revealed (Figure 2c) a single reflection located at $2\theta = 20.3°$ with an amorphous phase over to a highly crystalline region, which is in agreement with the literature [26,27]. The predominant amorphous character can be related to the breakage of hydrogen bonds in the crystalline region of cellulose starting material, along with the electrostatic interactions between the CMC compounds due to the anionic—CH2COO—groups [26]. Besides the clear amorphousness of the four CMC samples, the %CI was determined to attain the crystallinity extent of the different samples. The %CI calculation was performed on the PDXL2 da Rigaku® (version 2.8.1.1) software, after the adjustment of the diffractogram profile and the baseline, considering the area measurement under the single reflection,

followed by the modelling of the amorphous background. Then, the area corresponding to the crystalline component was obtained by the subtraction of the area of the amorphous background from the total area, with the %CI being obtained by the ratio between the area of crystalline and the total area. According to this analysis, CMC4 exhibited the higher crystallinity (42.1%), followed by CMC2 (40.6%), CMC3 (35.9%), and CMC1 (32.3%).

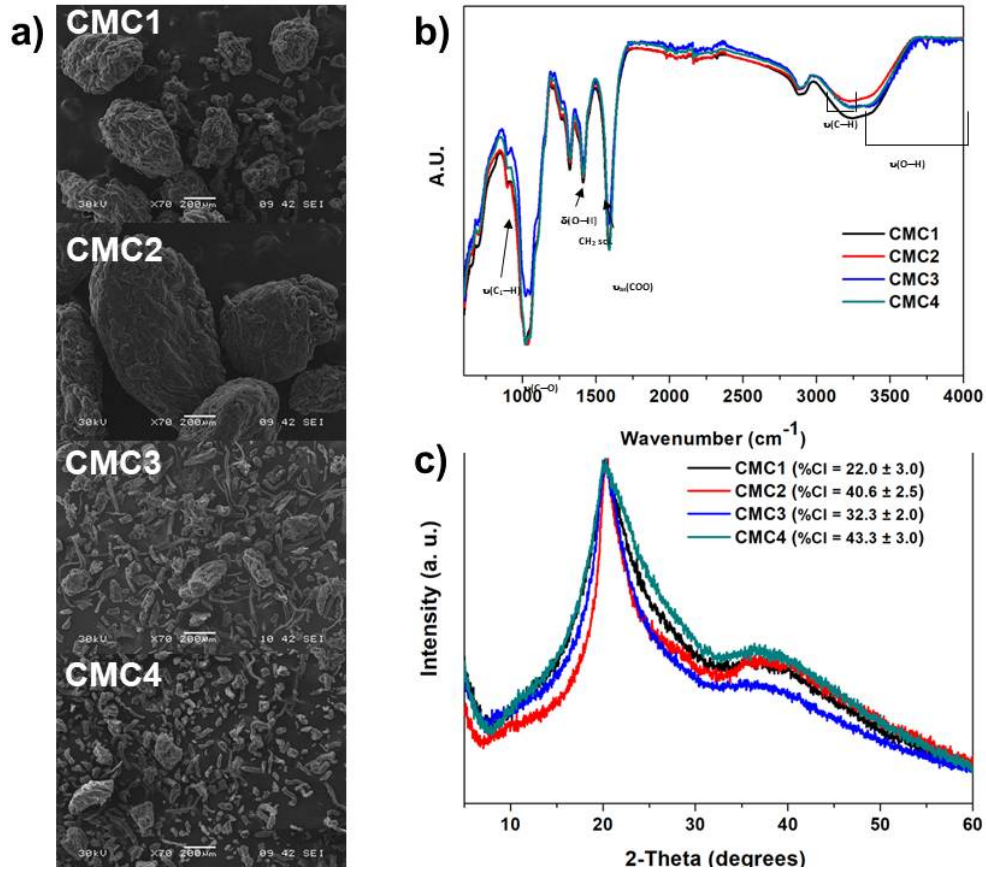

Figure 2. Structural characterization of CMC samples by (**a**) scanning electron microscopy, (**b**) Fourier-Transform Infrared Spectrometry, and (**c**) powder X-ray diffraction analysis.

The microstructure analysis of all CMC samples by SEM (Figure 2a) showed the presence of smooth particles aggregates. CMC2 exhibited the largest aggregates, followed by CMC 1, while the samples CMC3 and CMC4 seem to be very similar.

3.1.2. Physical Characterization

All CMC samples were characterized in terms of moisture content, purity degree, degree of substitution, and molar mass distribution, since these parameters may have an impact on the CMC biological properties. The data obtained are reported in Table 1.

Regarding sample purity, the results obtained showed that all CMC samples were highly pure (ranging from 97.23 to 99.61%) with no statistically significant differences ($p > 0.05$) being found between samples. The specification sheet of CMC2 reports the carbohydrate content of 93 ± 3% and the results obtained come in line with this information as they showed it possessed a purity degree of 97.23 ± 0.55%. Since no statistical differences ($p > 0.05$) were obtained among the samples and taking into consideration that the specification sheet of CMC2 (the CMC sample which showed the lowest purity) indicates that it complies with the regulation for purity requirements according to the commission directive 96/77/EC, BGBI.I.S.230 and BGBI.I.S.2082 standards, and FAO 1992, it was considered that all CMCs can be used for cosmetic, food, or pharmaceutical applications. In terms of moisture content, no statistical differences ($p > 0.05$) were found between CMC3 and CMC4

(5.09 and 5.97% respectively). On the other hand, CMC1 exhibited a statistically significantly lower ($p < 0.05$) moisture content (3.67%) and CMC2 a significantly higher ($p < 0.05$) moisture content (11.74%). The higher moisture content observed for CMC2 can be associated with the statistically higher ($p < 0.05$) M_w of this sample (i.e., 471.7 kDa) (Table 1) and the largest aggregates observed (Figure 1), which can bind more water molecules. It has been described as a proportional relationship between water absorption and M_w for cellulose derivative samples [28]. Another factor that can also contribute to the moisture protection is the crystallinity of CMC samples (Figure 2c), as materials with a higher crystalline state will typically have less water vapor sorption than the amorphous state, due to the reduction in free energy, void space, and/or surface area [29]. In this case, it was not possible to establish a clear relationship between the crystallinity degree and the moisture content of CMCs, and thus the M_w factor appeared to have a higher impact on the CMC water absorption.

Table 1. T Physical characteristics of the commercial CMCs evaluated. Different letters represent the statistically significant ($p < 0.05$) differences found between conditions.

Compound	Moisture (%)	Purity (%)	DS	Molar Mass Distribution		
				M_w (kDa)	Mn (kDa)	PI
CMC1	3.67 ± 0.19^{a}	99.61 ± 0.21^{a}	0.71 ± 0.03^{a}	370.1 ± 7.2^{a}	313.0 ± 6.3	1.2 ± 0.0
CMC2	11.74 ± 0.04^{b}	97.23 ± 0.55^{a}	0.80 ± 0.01^{b}	471.7 ± 1.0^{b}	382.6 ± 6.0	1.2 ± 0.0
CMC3	5.09 ± 0.12^{c}	99.55 ± 0.33^{a}	0.61 ± 0.01^{c}	407.0 ± 2.3^{c}	316.4 ± 3.7	1.3 ± 0.0
CMC4	5.97 ± 0.24^{c}	99.57 ± 0.25^{a}	0.71 ± 0.00^{a}	322.5 ± 9.0^{d}	288.9 ± 8.5	1.1 ± 0.0

Note: DS—degree of substitution; MW—weight-average molar mass; Mn—number-average molar mass; PI—polydispersity index. Different letters represent the statistically significant differences ($p < 0.05$) found between samples for the same condition.

These factors may also explain why CMC2 presented the largest particle aggregates in SEM imaging (Figure 2a). The product data sheets of samples CMC 1-2 reported a maximum moisture content of 10%, which was not experimentally verified, thus leading to a non-conformity, while the information available for CMC 3 reported a maximum of 8%. In the case of CMC4, we found a lack of information regarding this parameter. In the specific case of CMC1 and CMC3, it was possible to assess the certificates of analysis, where the values of moisture content of 2.9 and 6.3% were described, respectively. These values are in the line with those experimentally determined here, and thus in conformity with the maximum values defined. This parameter provides information about the water affinity of a material or its capacity to absorb water during powder processing and storage and thus is an important parameter to have in consideration since it significantly impacts the product's long-term stability and performance (e.g., compressibility, flowability, cohesion, caking, and density) [29].

The DS constitutes a pivotal property of CMC because it not only influences its solubility but also the solution characteristics, thus directly affecting the CMC physicochemical properties. By definition, DS is the average number of carboxymethyl groups per anhydroglucose unit. The DS range in the commercially available CMC samples is typically comprised between 0.4 and 1.5, with 3 being the maximum theoretical DS value [27]. The DS determined according to the ASTM D1439 standard [19] showed some differences between samples. For CMC1 and CMC4, no statistically significant ($p > 0.05$) differences were found with both samples presenting an average DS of 0.71. On the other hand, for CMC3 and CMC4 statistically significant ($p < 0.05$) differences were found, with CMC3 presenting the lowest DS (0.61) of all tested samples and CMC2 the highest (0.8). These data are in agreement with the information available in the product datasheets for CMC1 and CMC4 (0.79 and 0.70, respectively). In the case of CMC2, the product datasheet did not include this information, while for CMC3 the information stated that the DS range is between 0.75 and 0.85, which is significantly different from the result obtained here.

The molar mass distribution of CMC samples was determined using the standard curve for the molecular weight of polysaccharide patterns fromlinebreak ShodexTM [Log(MW) = −0.3615 (RT) + 10.162 with R2 of 0.981 (MW corresponds to the average molecular weight in Da, while RT is the retention time in minutes) and Equations (4)–(6). To obtain more rigorous data on the molar mass distribution, the chromatograms were sectioned and properly integrated. The results obtained according to Equation (4) showed that all samples had statistically significant ($p < 0.05$) different M_ws, with the average M_w of 370.1, 471.7, 407.0, and 322.5 KDa for CMC1, 2, 3, and 4, respectively. Generally, the increase in M_w led to an increase in viscosity of the aqueous solutions of CMC samples, which could have a negative impact on the biological properties studied due to the reduced availability of the CMC for interaction with different components in the cells.

3.1.3. Cytotoxicity Evaluation

When considering the effects of CMCs on the viability of the selected skin cell lines the results obtained can be seen in Figure 3.

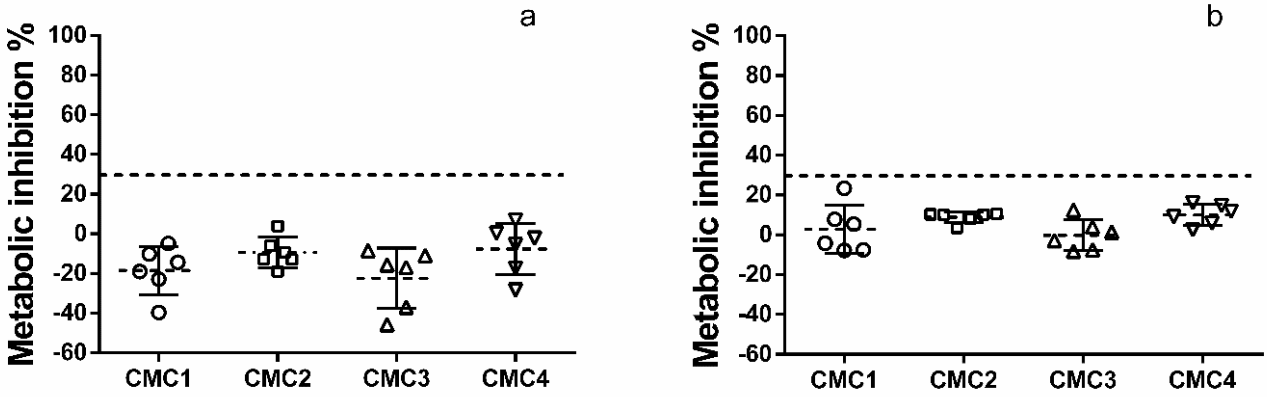

Figure 3. Cytotoxicity of CMCs towards HaCaT (**a**) and HDFa (**b**) cells. The dotted line represents the 30% cytotoxicity limit as defined by the ISO 10993-5:2009 standard.

For both cell lines, the studied CMCs cytotoxicity values were below the 30% threshold (dotted line) defined by the ISO 10993-5:2009 standard [30]. However, while no cytotoxicity was observed, it is interesting to see that for HaCaT cells (Figure 3a) the average metabolic inhibition was 0.14%, while for HDFa (Figure 3b) it was 5.39%. This difference is most likely due to the intrinsic differences between cell lines as fibroblasts are generally described as being more sensitive to compounds than keratinocytes [31–33].

The lack of cytotoxicity here observed has been previously described in the literature, as CMC in its various forms has been described as being non-cytotoxic against a variety of cell lines. For instance, CMC hydrogels have been shown to be safe towards human osteosarcoma-derived cells, HaCaT, primary mouse embryonic fibroblast, L929 mouse fibroblasts, and Vero cell line [6,34–38]. Similarly, CMC scaffolds for tissue engineering showed no cytotoxicity toward L929 cells, human chondrocytes, and osteosarcoma cells [9,39–41] and CMC nanostructures are safe toward fibroblasts, HEK293T, and HaCaT cells [42,43]. Additionally, anionic polysaccharides, due to their lack of direct interaction with cells, are usually regarded as non-cytotoxic toward human skin [44], as shown by Summa and Russo [45] who demonstrated that a 3% (w/v) alginate film was biocompatible with human foreskin fibroblasts, and by Pereira and Barrias [46] who showed that a 2.5 (w/v) pectin hydrogel had no cytotoxicity towards human neonatal dermal fibroblast.

3.1.4. Pro-Collagen I α I Production

Collagen, the most abundant protein found in humans, and the primary structural component of the dermis, is responsible for conferring strength and support to human skin. Alterations in collagen play an integral role in the ageing process. Type I collagen, the most abundant dermal collagen, is composed of two types of pro-collagen: pro-collagen I α I

and α 2 chains. Thus, by measuring the protein levels of pro-collagen I α I it is possible to estimate alterations in the levels of collagen type I [47,48], which may be a critical step toward the development of any possible cosmetic ingredient.

With regards to the effects of CMC upon pro-collagen, I α I production, the first step was the quantification of the protein content of the cellular extracts obtained. As can be seen from Figure 4, CMC2 and CMC4 significantly ($p < 0.05$) reduced the total protein content recovered from HDFa cells.

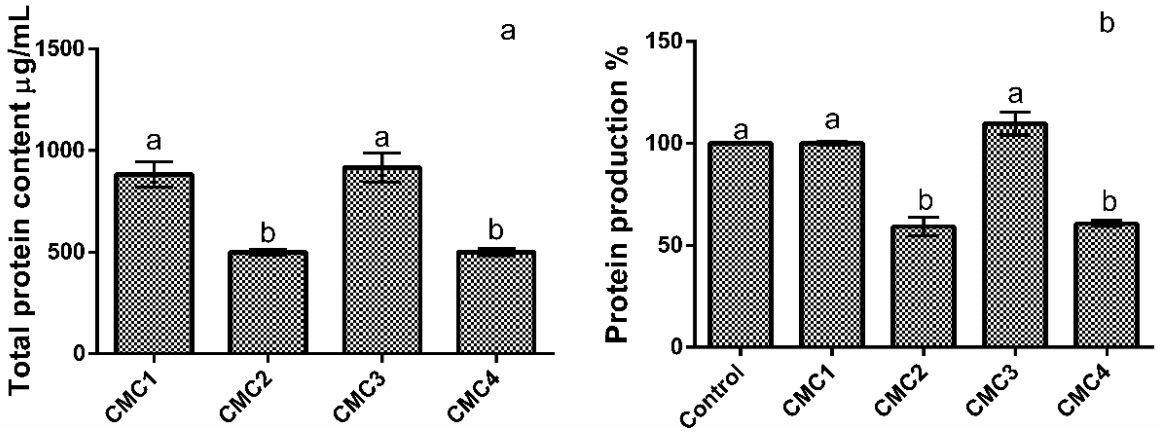

Figure 4. Total protein content of HDFa cells in the presence of CMC. (**a**) Total protein content; (**b**) percentage of protein production relative to the basal level (control). Different letters represent the statistically significant differences ($p < 0.05$) found between conditions.

However, considering the lack of impact on the cellular metabolism previously observed, it is most likely that the reductions here observed are a result of protein adsorption by the CMC fibers, as previous works described that anionic polymers, such as CMC, are capable of adsorbing biomolecules [49–51]. As to why only two of the four CMC samples assayed displayed this behavior, the most likely explanation is the crystallinity index. Considering that both samples had a higher crystallinity index and that, as previously shown, higher crystallinity indexes are usually associated with higher degrees of interaction with biological molecules, it is only natural that these samples will have higher protein adsorption properties [52,53].

When analyzing the results regarding the pro-collagen I α I production (Figure 5), one can see that CMC was only capable of modulating intracellular production (Figure 5a) and not extracellular (Figure 5b).

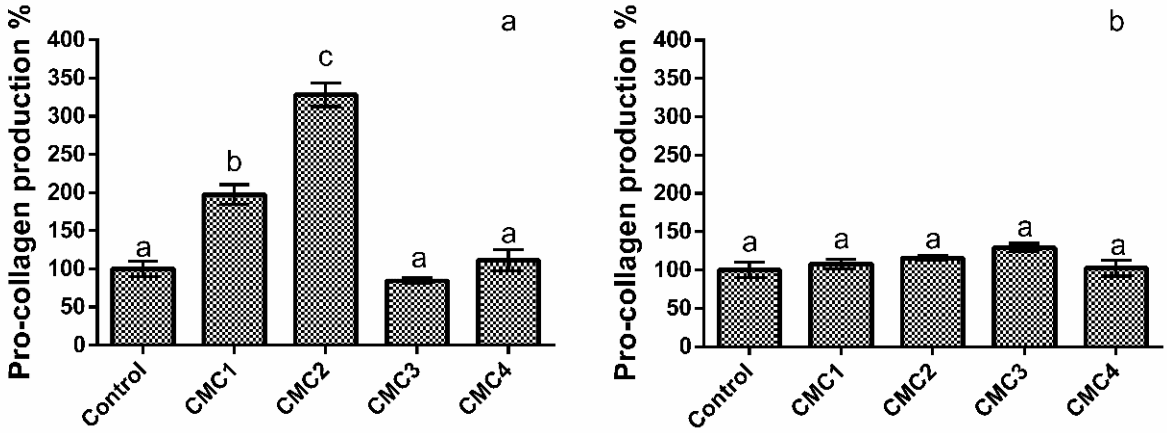

Figure 5. Pro-collagen I α I relative percentage of production in the presence of different CMC samples relative to the basal level (control). (**a**) Intracellular; (**b**) extracellular. Different letters represent the statistically significant differences ($p < 0.05$) found between conditions.

This discrepancy may be a result of the addition of CMC to the culture media which may alter the reaction kinetics of collagen assembly and increase the deposition of collagen in the extracellular matrix, a phenomenon previously described by Shendi and Marzi [54]. A similar explanation can be a mechanism similar to the steric hindrance of fibril formation reported by Smith and Hunt [55] for an alginate hydrogel, in which pro-collagen was observed in the pericellular space, but was not present in the extracellular matrix due to basically a lack of space for lateral fibril growth. Additionally, authors Mesquida and Kohl [56] and Wu and Liu [57] have previously described cationic collagen as being adsorbed to CMC through interactions with its -COOH group. It is likely that the lack of modulation observed in the extracellular setting was a consequence of this interaction and not a lack of activity of CMC samples. This hypothesis has been recently confirmed by Dalir Abdolahinia and Jafari [58], who showed through docking analysis that CMC interacted with the Lys, Thr, and Pro amino acids present in collagen through hydrogen bonds and van der Waals and that the affinity for said interaction was high as it had a low energy.

When considering only the intracellular data (Figure 5a), one can see that only two samples (CMC1 and CMC2) significantly ($p < 0.05$) modulated collagen production with CMC2 increasing collagen production by ca. 228% relative to the basal level of production in the control. When considering the intrinsic properties of the CMC molecules assayed, it is interesting to see that the highest pro-collagen I α I productions were obtained for CMC2 which showed the highest DS and M_w. Moreover, sample crystallinity does not appear to be a differentiating factor between these samples, as CMC4 had the highest crystallinity index of all samples assayed and produced an increase of only 11% in pro-collagen I α I production. While the lack of previous works on this topic makes reaching any definitive explanation for this behavior difficult, some analysis can still be performed with support from the literature. In line with what was discussed here, Choi, Hwang [59] reported that levan, pluronic, and CMC hydrogel enhanced collagen production in human fibroblasts. Similarly, P.B and S [60] showed that a complex CMC scaffold led to increases in collagen production from osteosarcoma cells. Another fact to take into consideration is that bacterial cellulose has been shown to stimulate Type I collagen production both as a scaffold and as a hydrogel [61,62]. If one disregards the intrinsic differences between molecules—bacterial cellulose is composed of type I cellulose with a parallel arrangement of chains and is more crystalline than CMC, which is composed of type II cellulose with an antiparallel arrangement of chains and lower crystallinity—it is possible that still unknown intrinsic properties of cellulose may be at play [52,63–65].

3.1.5. Interleukins Production

While inflammatory processes in the skin are widely associated with skin inflammatory diseases (such as psoriasis and atopic dermatitis), they also play a key role in UV protection and wound healing [66,67]. In the first, UV exposure causes acute phase responses that stimulate inflammatory factors such as IL-6 and IL-8. The second interleukins, and IL-8 in particular, are one of the most important regulators of wound healing, epithelial regeneration, and angiogenesis [65,68]. The results obtained for the interleukins production (Figures 6 and 7) showed that, for IL-6 (Figure 6), while all CMC samples had a pro-inflammatory effect upon HaCaT cells, only CMC3 had a stronger pro-inflammatory activity than the LPS control. On the other hand, regarding IL-8 production (Figure 7), the results obtained showed that all CMC samples tested significantly ($p < 0.05$) reduced IL-8 levels in comparison to the basal control.

When analyzing a possible impact of CMC's intrinsic characteristics upon the data obtained, the first major takeaway is that for IL-8 (Figure 7) no factor bears any significant ($p > 0.05$) weight on the samples' displayed activity. In contrast, data obtained regarding IL-6 (Figure 6) presented a complex pattern of response linked to the DS and crystallinity of the samples. CMC samples' DS appears to influence IL-6 levels, as samples with the lowest DS produced the highest inflammatory response. However, when the DS was above 0.7, sample crystallinity appears to play a significant role, as while both CMC1 and CMC4

have the same DS, CMC4, which has a higher crystallinity index, produced a significantly ($p < 0.05$) lower inflammatory response.

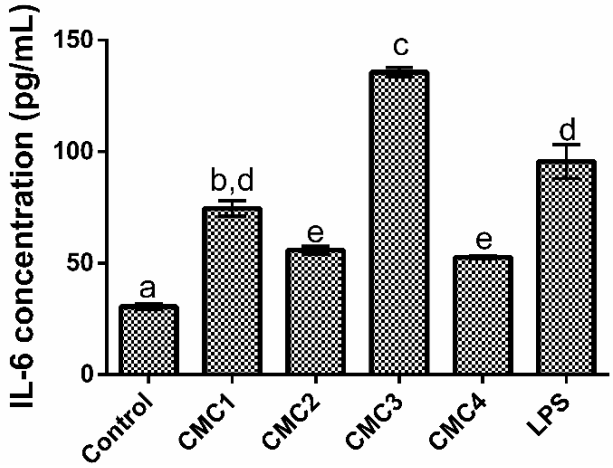

Figure 6. IL-6 production in HaCaT cells in the presence of CMC relative to the basal level (control). Different letters represent the statistically significant differences ($p < 0.05$) found between conditions.

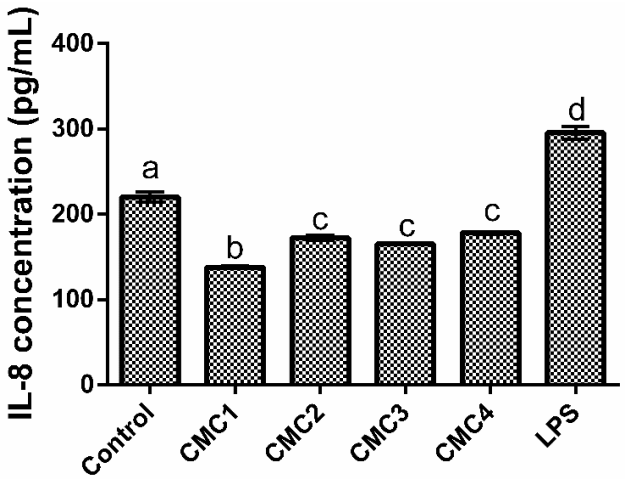

Figure 7. IL-8 production in HaCaT cells in the presence of CMC relative to the basal level (control). Different letters represent the statistically significant differences ($p < 0.05$) found between conditions.

When considering the impact of CMCs upon these specific interleukins' production, no previous works exist that may allow for a direct comparison; however, this does not mean that discussion of the data generated is not possible. When looking into the general effect of CMC on the inflammatory response of cells the existing body of work depicts carboxymethyl cellulose as being, in general, non-inflammatory. Nayak and Kundu [69], showed that CMC had no pro-inflammatory activity upon HaCaT cells as no increase in the production of TNF-α was detected. Similarly, Kollar and Závalová [70] reported CMC as not being pro-inflammatory toward THP-1 cells. Additionally, Nordli and Chinga-Carrasco [43] showed that cellulose nanofibers reduced IL-6 production in HaCaT cells and, while CMC was not at play here, this interaction shows that, in principle, cellulose-based molecules should not have a pro-inflammatory activity. While all of the previous works support the results here obtained for IL-8, they are contrary to those obtained for IL-6. A possible explanation for this discrepancy may be found in the work of Lopes and Sanchez-Martinez [50], as the authors showed that the introduction of the carboxymethyl group in cellulose nanofibrils had a pro-inflammatory effect. However, the lack of information regarding CMCs characteristics in these works makes identifying any responsible characteristic or defining any pattern of activity very difficult, and as such, further assays

are required to better understand CMCs' pro- or anti-inflammatory potential towards HaCaT cells.

Last but not least, the increase in IL-6 production observed may be a double-edged sword. On the one hand, IL-6 production by HaCaT has been shown to be able to stimulate fibroblast proliferation; on the other hand, IL-6 production in HaCaT cells has been developed as a non-animal alternative to determine a chemical's skin sensitizing potential [71,72]. Considering the results here obtained, all samples may to some extent possess some skin sensitization potential. However, as this assay is only one of four key events defined by the OECD to assess skin sensitization and only a positive result in two or more of those events leads to a positive outcome, no conclusions regarding this topic can be reached at this point [73,74].

4. Conclusions

A comprehensive analysis of work performed led to the conclusion that the proposed hypothesis was supported by the data reported in this work, and, as such, CMC showed significant potential for future incorporation into skincare products not only as a structural component but also as a bioactive one. While all the samples were shown to be capable of modulating pro-collagen I-α-I metabolism, only CMC2 showed the largest potential for incorporation in future products. In fact, this CMC was not cytotoxic up to 10 mg/mL for both HaCaT and HDFa and at this concentration led to increases in pro-collagen I-α-I of 228% relative to the basal metabolism. Interestingly, this CMC sample had the highest DS and M*w* of all tested CMCs, which seems to indicate a possible correlation between these parameters and the observed biological modulation. Furthermore, when considering the impact of these samples upon HaCaT inflammatory metabolism, CMC2 was once again the best performing sample, as while all samples led to increases in the secretion of IL-6, CMC2 led to the lowest promotion of this cytokine. Curiously, for IL-8 secretion a completely different behavior was observed as all samples led to reductions in IL-8 production in the studied conditions. These results, while noteworthy, still require further assays to better understand CMC's potential in modulating skincare relevant molecules and in understanding the role of CMC in the immune response of skin associated cells.

Author Contributions: Conceptualization, E.M.C. and O.L.R.; methodology, E.M.C. and C.F.P.; investigation: E.M.C., C.F.P., A.A.R., F.C. and R.F.; validation, E.M.C., C.F.P. and O.L.R.; writing—original draft preparation, E.M.C. and C.F.P.; writing—review and editing, O.L.R. and M.P.; supervision, O.L.R. and M.P.; funding acquisition, M.P. All authors have read and agreed to the published version of the manuscript.

Funding: This research was funded by FCT—Fundação para a Ciência e a Tecnologia, grant number UIDB/50016/2020 and by AICEP, grant number POCI-01-0247-FEDER-027578.

Institutional Review Board Statement: Not applicable.

Informed Consent Statement: Not applicable.

Data Availability Statement: The data presented in this study are available on request from the corresponding author. The data are not publicly available due to confidentiality agreements.

Acknowledgments: The authors thank João Silva for the experimental support in immunostimulant assay, and Joana Durão and Manuela Amorim for the experimental support on the molar mass distribution analyses.

Conflicts of Interest: The authors declare no conflict of interest.

References

1. Golbaghi, L.; Khamforoush, M.; Hatami, T. Carboxymethyl cellulose production from sugarcane bagasse with steam explosion pulping: Experimental, modeling, and optimization. *Carbohydr. Polym.* **2017**, *174*, 780–788. [CrossRef]
2. Rahman, M.; Hasan, M.; Nitai, A.S.; Nam, S.; Karmakar, A.K.; Ahsan, M.; Shiddiky, M.J.; Ahmed, M.B. Recent Developments of Carboxymethyl Cellulose. *Polymers* **2021**, *13*, 1345. [CrossRef] [PubMed]

3. Shui, T.; Feng, S.; Chen, G.; Li, A.; Yuan, Z.; Shui, H.; Kuboki, T.; Xu, C. Synthesis of sodium carboxymethyl cellulose using bleached crude cellulose fractionated from cornstalk. *Biomass Bioenergy* **2017**, *105*, 51–58. [CrossRef]
4. Toğrul, H.; Arslan, N. Production of carboxymethyl cellulose from sugar beet pulp cellulose and rheological behaviour of carboxymethyl cellulose. *Carbohydr. Polym.* **2003**, *54*, 73–82. [CrossRef]
5. Lakshmi, D.S.; Trivedi, N.; Reddy, C.R.K. Synthesis and characterization of seaweed cellulose derived carboxymethyl cellulose. *Carbohydr. Polym.* **2017**, *157*, 1604–1610. [CrossRef]
6. Sadeghi, S.; Nourmohammadi, J.; Ghaee, A.; Soleimani, N. Carboxymethyl cellulose-human hair keratin hydrogel with controlled clindamycin release as antibacterial wound dressing. *Int. J. Biol. Macromol.* **2020**, *147*, 1239–1247. [CrossRef]
7. Candido, R.; Gonçalves, A. Synthesis of cellulose acetate and carboxymethylcellulose from sugarcane straw. *Carbohydr. Polym.* **2016**, *152*, 679–686. [CrossRef]
8. Karataş, M.; Arslan, N. Flow behaviours of cellulose and carboxymethyl cellulose from grapefruit peel. *Food Hydrocoll.* **2016**, *58*, 235–245. [CrossRef]
9. Sharmila, G.; Muthukumaran, C.; Kirthika, S.; Keerthana, S.; Kumar, N.M.; Jeyanthi, J. Fabrication and characterization of Spinacia oleracea extract incorporated alginate/carboxymethyl cellulose microporous scaffold for bone tissue engineering. *Int. J. Biol. Macromol.* **2020**, *156*, 430–437. [CrossRef]
10. Matinfar, M.; Mesgar, A.S.; Mohammadi, Z. Evaluation of physicochemical, mechanical and biological properties of chitosan/carboxymethyl cellulose reinforced with multiphasic calcium phosphate whisker-like fibers for bone tissue engineering. *Mater. Sci. Eng. C* **2019**, *100*, 341–353. [CrossRef]
11. Wang, X.; Mo, X. High Hygroscopic Wound Dressing and Preparation Method and Use Thereof. C.N. Patent PCT/CN2013/082801, 2 September 2013.
12. Yan, M.; Chen, T.; Zhang, S.; Lu, T.; Sun, X. A core-shell structured alginate hydrogel beads with tunable thickness of carboxymethyl cellulose coating for pH responsive drug delivery. *J. Biomater. Sci. Polym. Ed.* **2021**, *32*, 763–778. [CrossRef] [PubMed]
13. Doucet, O.; Bernini, D.; Robert, C.; Pujos, M. Cosmetic with Enhanced Collagen i Synthesis. European Patent EP12745428.8A, 14 July 2014.
14. Gawade, R.P.; Chinke, S.L.; Alegaonkar, P.S. Chapter 17—Polymers in cosmetics. In *Polymer Science and Innovative Applications*; AlMaadeed, M.A.A., Ponnamma, D., Carignano, M.A., Eds.; Elsevier: Amsterdam, The Netherlands, 2020; pp. 545–565.
15. Martins, D.; Rocha, C.; Dourado, F.; Gama, M. Bacterial Cellulose-Carboxymethyl Cellulose (BC:CMC) dry formulation as stabilizer and texturizing agent for surfactant-free cosmetic formulations. *Colloids Surf. Physicochem. Eng. Asp.* **2021**, *617*, 126380. [CrossRef]
16. Mitura, S.; Sionkowska, A.; Jaiswal, A. Biopolymers for hydrogels in cosmetics: Review. *J. Mater. Sci. Mater. Med.* **2020**, *31*, 50. [CrossRef]
17. Alves, T.F.R.; Morsink, M.; Batain, F.; Chaud, M.V.; Almeida, T.; Fernandes, D.A.; da Silva, C.F.; Souto, E.B.; Severino, P. Applications of Natural, Semi-Synthetic, and Synthetic Polymers in Cosmetic Formulations. *Cosmetics* **2020**, *7*, 75. [CrossRef]
18. Wongkom, L.; Jimtaisong, A. Novel biocomposite of carboxymethyl chitosan and pineapple peel carboxymethylcellulose as sunscreen carrier. *Int. J. Biol. Macromol.* **2017**, *95*, 873–880. [CrossRef]
19. *ASTM D1439-03*; Standard Test Methods for Sodium Carboxymethylcellulose. ASTM International: West Conshohocken, PA, USA, 2016; p. 9.
20. Condezo-Hoyos, L.; Pérez-López, E.; Rupérez, P. Improved evaporative light scattering detection for carbohydrate analysis. *Food Chem.* **2015**, *180*, 265–271. [CrossRef]
21. Baik, Y.-S.; Cheong, W.-J. Determination of molecular weight distribution and average molecular weights of oligosaccharides by HPLC with a common C18 phase and a mobile phase with high water content. *Bull. Korean Chem. Soc.* **2007**, *28*, 847–850.
22. Melander, M.; Vuorinen, T. Determination of the degree of polymerisation of carboxymethyl cellulose by size exclusion chromatography. *Carbohydr. Polym.* **2001**, *46*, 227–233. [CrossRef]
23. Costa, E.M.; Silva, S.; Veiga, M.; Baptista, P.; Tavaria, F.K.; Pintado, M.E. Textile dyes loaded chitosan nanoparticles: Characterization, biocompatibility and staining capacity. *Carbohydr. Polym.* **2021**, *251*, 117120. [CrossRef]
24. Chua, K.Y.; Azzahari, A.D.; Abouloula, C.N.; Sonsudin, F.; Shahabudin, N.; Yahya, R. Cellulose-based polymer electrolyte derived from waste coconut husk: Residual lignin as a natural plasticizer. *J. Polym. Res.* **2020**, *27*, 115. [CrossRef]
25. Morán, J.I.; Alvarez, V.A.; Cyras, V.P.; Vázquez, A. Extraction of cellulose and preparation of nanocellulose from sisal fibers. *Cellulose* **2008**, *15*, 149–159. [CrossRef]
26. Pushpamalar, V.; Langford, S.J.; Ahmad, M.; Lim, Y.Y. Optimization of reaction conditions for preparing carboxymethyl cellulose from sago waste. *Carbohydr. Polym.* **2006**, *64*, 312–318. [CrossRef]
27. Doh, S.J.; Lee, J.Y.; Lim, D.Y.; Im, J.N. Manufacturing and analyses of wet-laid nonwoven consisting of carboxymethyl cellulose fibers. *Fibers Polym.* **2013**, *14*, 2176–2184. [CrossRef]
28. Shlieout, G.; Arnold, K.; Müller, G. Powder and mechanical properties of microcrystalline cellulose with different degrees of polymerization. *AAPS PharmSciTech* **2002**, *3*, 45–54. [CrossRef] [PubMed]
29. Yu, J.; Romeo, M.-C.; Cavallaro, A.A.; Chan, H.-K. Protective effect of sodium stearate on the moisture-induced deterioration of hygroscopic spray-dried powders. *Int. J. Pharm.* **2018**, *541*, 11–18. [CrossRef]

30. *ISO 10993-5:2009*; Biological Evaluation of Medical Devices, in Part 5: Tests for in Vitro Cytotoxicity. International Organization for Standardization: Geneva, Switzerland, 2009; p. 34.
31. Moharamzadeh, K.; Van Noort, R.; Brook, I.M.; Scutt, A.M. Cytotoxicity of resin monomers on human gingival fibroblasts and HaCaT keratinocytes. *Dent. Mater.* **2007**, *23*, 40–44. [CrossRef]
32. Damour, O.; Hua, S.Z.; Lasne, F.; Villain, M.; Rousselle, P.; Collombel, C. Cytotoxicity evaluation of antiseptics and antibiotics on cultured human fibroblasts and keratinocytes. *Burns* **1992**, *18*, 479–485. [CrossRef]
33. Wiegand, C.; Hipler, U.-C. Evaluation of biocompatibility and cytotoxicity using keratinocyte and fibroblast cultures. *Ski. Pharmacol. Physiol.* **2009**, *22*, 74–82. [CrossRef]
34. Shah, R.; Saha, N.; Kuceková, Z.; Humpolicek, P.; Saha, P. Properties of biomineralized (CaCO3) PVP-CMC hydrogel with reference to its cytotoxicity. *Int. J. Polym. Mater. Polym. Biomater.* **2016**, *65*, 619–628. [CrossRef]
35. Roy, N.; Saha, N.; Humpolicek, P.; Saha, P. Permeability and biocompatibility of novel medicated hydrogel wound dressings. *Soft Mater.* **2010**, *8*, 338–357. [CrossRef]
36. Capanema, N.S.; Mansur, A.A.; Mansur, H.S.; de Jesus, A.C.; Carvalho, S.M.; Chagas, P.; de Oliveira, L.C. Eco-friendly and biocompatible cross-linked carboxymethylcellulose hydrogels as adsorbents for the removal of organic dye pollutants for environmental applications. *Environ. Technol.* **2018**, *39*, 2856–2872. [CrossRef] [PubMed]
37. Chantereau, G.; Sharma, M.; Abednejad, A.; Vilela, C.; Costa, E.; Veiga, M.; Antunes, F.; Pintado, M.; Sèbe, G.; Coma, V. Bacterial nanocellulose membranes loaded with vitamin B-based ionic liquids for dermal care applications. *J. Mol. Liq.* **2020**, *302*, 112547. [CrossRef]
38. Turky, G.; Moussa, M.A.; Hasanin, M.; El-Sayed, N.S.; Kamel, S. Carboxymethyl Cellulose-Based Hydrogel: Dielectric Study, Antimicrobial Activity and Biocompatibility. *Arab. J. Sci. Eng.* **2021**, *46*, 17–30. [CrossRef]
39. Kundu, J.; Mohapatra, R.; Kundu, S. Silk fibroin/sodium carboxymethylcellulose blended films for biotechnological applications. *J. Biomater. Sci. Polym. Ed.* **2011**, *22*, 519–539. [CrossRef] [PubMed]
40. Namkaew, J.; Sawaddee, N.; Yodmuang, S. Polyvinyl Alcohol-Carboxymethyl Cellulose Scaffolds for Cartilage Tissue Formation. In Proceedings of the 2019 12th Biomedical Engineering International Conference (BMEiCON), Ubon Ratchathani, Thailand and Pakse, Laos, 19–22 November 2019.
41. Priya, G.; Madhan, B.; Narendrakumar, U.; Suresh Kumar, R.V.; Manjubala, I. In Vitro and In Vivo Evaluation of Carboxymethyl Cellulose Scaffolds for Bone Tissue Engineering Applications. *ACS Omega* **2021**, *6*, 1246–1253. [CrossRef]
42. Capanema, N.S.; Mansur, A.A.; Carvalho, S.M.; Mansur, L.L.; Ramos, C.P.; Lage, A.P.; Mansur, H.S. Physicochemical properties and antimicrobial activity of biocompatible carboxymethylcellulose-silver nanoparticle hybrids for wound dressing and epidermal repair. *J. Appl. Polym. Sci.* **2018**, *135*, 45812. [CrossRef]
43. Nordli, H.R.; Chinga-Carrasco, G.; Rokstad, A.M.; Pukstad, B. Producing ultrapure wood cellulose nanofibrils and evaluating the cytotoxicity using human skin cells. *Carbohydr. Polym.* **2016**, *150*, 65–73. [CrossRef]
44. Fattahi, A.; Petrini, P.; Munarin, F.; Shokoohinia, Y.; Golozar, M.A.; Varshosaz, J.; Tanzi, M.C. Polysaccharides derived from tragacanth as biocompatible polymers and gels. *J. Appl. Polym. Sci.* **2013**, *129*, 2092–2102. [CrossRef]
45. Summa, M.; Russo, D.; Penna, I.; Margaroli, N.; Bayer, I.S.; Bandiera, T.; Athanassiou, A.; Bertorelli, R. A biocompatible sodium alginate/povidone iodine film enhances wound healing. *Eur. J. Pharm. Biopharm.* **2018**, *122*, 17–24. [CrossRef]
46. Pereira, R.F.; Barrias, C.C.; Bártolo, P.J.; Granja, P.L. Cell-instructive pectin hydrogels crosslinked via thiol-norbornene photo-click chemistry for skin tissue engineering. *Acta Biomater.* **2018**, *66*, 282–293. [CrossRef]
47. Ogen-Shtern, N.; Chumin, K.; Cohen, G.; Borkow, G. Increased pro-collagen 1, elastin, and TGF-β1 expression by copper ions in an ex-vivo human skin model. *J. Cosmet. Dermatol.* **2020**, *19*, 1522–1527. [CrossRef] [PubMed]
48. Baumann, L. Skin ageing and its treatment. *J. Pathol. A J. Pathol. Soc. Great Br. Irel.* **2007**, *211*, 241–251. [CrossRef] [PubMed]
49. Hasan, A.; Waibhaw, G.; Saxena, V.; Pandey, L.M. Nano-biocomposite scaffolds of chitosan, carboxymethyl cellulose and silver nanoparticle modified cellulose nanowhiskers for bone tissue engineering applications. *Int. J. Biol. Macromol.* **2018**, *111*, 923–934. [CrossRef] [PubMed]
50. Lopes, V.R.; Sanchez-Martinez, C.; Strømme, M.; Ferraz, N. In vitro biological responses to nanofibrillated cellulose by human dermal, lung and immune cells: Surface chemistry aspect. *Part. Fibre Toxicol.* **2017**, *14*, 1. [CrossRef]
51. Kono, H. Characterization and properties of carboxymethyl cellulose hydrogels crosslinked by polyethylene glycol. *Carbohydr. Polym.* **2014**, *106*, 84–93. [CrossRef]
52. Hickey, R.J.; Pelling, A.E. Cellulose biomaterials for tissue engineering. *Front. Bioeng. Biotechnol.* **2019**, *7*, 45. [CrossRef]
53. Areias, A.; Ribeiro, C.; Sencadas, V.; García-Giralt, N.; Diez-Perez, A.; Ribelles, J.G.; Lanceros-Méndez, S. Influence of crystallinity and fiber orientation on hydrophobicity and biological response of poly (l-lactide) electrospun mats. *Soft Matter* **2012**, *8*, 5818–5825. [CrossRef]
54. Shendi, D.; Marzi, J.; Linthicum, W.; Rickards, A.; Dolivo, D.; Keller, S.; Kauss, M.; Wen, Q.; McDevitt, T.; Dominko, T. Hyaluronic acid as a macromolecular crowding agent for production of cell-derived matrices. *Acta Biomater.* **2019**, *100*, 292–305. [CrossRef]
55. Smith, A.M.; Hunt, N.C.; Shelton, R.M.; Birdi, G.; Grover, L.M. Alginate hydrogel has a negative impact on in vitro collagen 1 deposition by fibroblasts. *Biomacromolecules* **2012**, *13*, 4032–4038. [CrossRef]
56. Mesquida, P.; Kohl, D.; Andriotis, O.G.; Thurner, P.J.; Duer, M.; Bansode, S.; Schitter, G. Evaluation of surface charge shift of collagen fibrils exposed to glutaraldehyde. *Sci. Rep.* **2018**, *8*, 10126. [CrossRef]

57. Wu, J.; Liu, F.; Yu, Z.; Ma, Y.; Goff, H.D.; Ma, J.; Zhong, F. Facile preparation of collagen fiber–glycerol-carboxymethyl cellulose composite film by immersing method. *Carbohydr. Polym.* **2020**, *229*, 115429. [CrossRef] [PubMed]
58. Dalir Abdolahinia, E.; Jafari, B.; Parvizpour, S.; Barar, J.; Nadri, S.; Omidi, Y. Role of cellulose family in fibril organization of collagen for forming 3D cancer spheroids: In vitro and in silico approach. *BioImpacts BI* **2021**, *11*, 111–117. [CrossRef] [PubMed]
59. Choi, W.I.; Hwang, Y.; Sahu, A.; Min, K.; Sung, D.; Tae, G.; Chang, J.H. An injectable and physical levan-based hydrogel as a dermal filler for soft tissue augmentation. *Biomater. Sci.* **2018**, *6*, 2627–2638. [CrossRef] [PubMed]
60. Sathish, P.B.; Gayathri, S.; Priyanka, J.; Muthusamy, S.; Narmadha, R.; Krishnakumar, G.S.; Selvakumar, R. Tricomposite gelatin-carboxymethylcellulose-alginate bioink for direct and indirect 3D printing of human knee meniscal scaffold. *Int. J. Biol. Macromol.* **2022**, *195*, 179–189.
61. Brackmann, C.; Zaborowska, M.; Sundberg, J.; Gatenholm, P.; Enejder, A. In situ imaging of collagen synthesis by osteoprogenitor cells in microporous bacterial cellulose scaffolds. *Tissue Eng. Methods* **2012**, *18*, 227–234. [CrossRef]
62. Mohamad, N.; Loh, E.Y.X.; Fauzi, M.B.; Ng, M.H.; Mohd Amin, M.C.I. In vivo evaluation of bacterial cellulose/acrylic acid wound dressing hydrogel containing keratinocytes and fibroblasts for burn wounds. *Drug Deliv. Transl. Res.* **2019**, *9*, 444–452. [CrossRef]
63. Feng, X.; Ullah, N.; Wang, X.; Sun, X.; Li, C.; Bai, Y.; Chen, L.; Li, Z. Characterization of bacterial cellulose by Gluconacetobacter hansenii CGMCC 3917. *J. Food Sci.* **2015**, *80*, E2217–E2227. [CrossRef]
64. Hayakawa, D.; Nishiyama, Y.; Mazeau, K.; Ueda, K. Evaluation of hydrogen bond networks in cellulose Iβ and II crystals using density functional theory and Car–Parrinello molecular dynamics. *Carbohydr. Res.* **2017**, *449*, 103–113. [CrossRef]
65. Casaburi, A.; Rojo, Ú.M.; Cerrutti, P.; Vázquez, A.; Foresti, M.L. Carboxymethyl cellulose with tailored degree of substitution obtained from bacterial cellulose. *Food Hydrocoll.* **2018**, *75*, 147–156. [CrossRef]
66. Tang, S.-C.; Liao, P.-Y.; Hung, S.-J.; Ge, J.-S.; Chen, S.-M.; Lai, J.-C.; Hsiao, Y.-P.; Yang, J.-H. Topical application of glycolic acid suppresses the UVB induced IL-6, IL-8, MCP-1 and COX-2 inflammation by modulating NF-κB signaling pathway in keratinocytes and mice skin. *J. Dermatol. Sci.* **2017**, *86*, 238–248. [CrossRef]
67. Esquivel-García, R.; Ayiania, M.; Abu-Lail, N.; López-Meza, J.E.; Rosa, E.; García-Pérez, M.; Ochoa-Zarzosa, A.; García-Pérez, M.-E. Pyrolytic oils from Amphipterygium adstringens bark inhibit IL-8 production of IL-17-stimulated HaCaT keratinocytes. *J. Anal. Appl. Pyrolysis* **2020**, *145*, 104749. [CrossRef]
68. Lembo, S.; Balato, A.; Di Caprio, R.; Cirillo, T.; Giannini, V.; Gasparri, F.; Monfrecola, G. The modulatory effect of ellagic acid and rosmarinic acid on ultraviolet-B-induced cytokine/chemokine gene expression in skin keratinocyte (HaCaT) cells. *BioMed Res. Int.* **2014**, *2014*, 346793. [CrossRef] [PubMed]
69. Nayak, S.; Kundu, S. Sericin–carboxymethyl cellulose porous matrices as cellular wound dressing material. *J. Biomed. Mater. Res. Part A* **2014**, *102*, 1928–1940. [CrossRef] [PubMed]
70. Kollar, P.; Závalová, V.; Hošek, J.; Havelka, P.; Sopuch, T.; Karpíšek, M.; Třetinová, D.; Suchý Jr, P. Cytotoxicity and effects on inflammatory response of modified types of cellulose in macrophage-like THP-1 cells. *Int. Immunopharmacol.* **2011**, *11*, 997–1001. [CrossRef] [PubMed]
71. Peng, S.; Liu, W.; Han, B.; Chang, J.; Li, M.; Zhi, X. Effects of carboxymethyl-chitosan on wound healing in vivo and in vitro. *J. Ocean Univ. China* **2011**, *10*, 369–378. [CrossRef]
72. Jeon, B.; Kim, M.O.; Kim, Y.-S.; Han, H.-Y.; Yun, J.-H.; Kim, J.; Huang, Y.; Choi, Y.; Cho, C.-H.; Kang, B.-C. Optimization and validation of a method to identify skin sensitization hazards using IL-1 α and IL-6 secretion from HaCaT. *Toxicol. Vitr.* **2019**, *61*, 104589. [CrossRef]
73. OECD. *The Adverse Outcome Pathway for Skin Sensitisation Initiated by Covalent Binding to Proteins*; OECD Publishing: Paris, France, 2014.
74. Kleinstreuer, N.C.; Hoffmann, S.; Alépée, N.; Allen, D.; Ashikaga, T.; Casey, W.; Clouet, E.; Cluzel, M.; Desprez, B.; Gellatly, N. Non-animal methods to predict skin sensitization (II): An assessment of defined approaches. *Crit. Rev. Toxicol.* **2018**, *48*, 359–374. [CrossRef]